

Total oxidation of propene and propane over gold–copper oxide on alumina catalysts Comparison with Pt/Al₂O₃

Andreea C. Gluhoi^a, Nina Bogdanchikova^b, Bernard E. Nieuwenhuys^{a,*}

^aDepartment of Heterogeneous Catalysis and Surface Chemistry, Leiden Institute of Chemistry, Leiden University,
P.O. Box 9502, 2300 RA Leiden, The Netherlands

^bCentro de Ciencias de la Materia Condensada, UNAM, Km. 107, Carretera Tijuana-Ensenada,
22800 Ensenada, Baja California, Mexico

Available online 6 January 2006

Abstract

Oxidation of propene and propane to CO₂ and H₂O has been studied over Au/Al₂O₃ and two different Au/CuO/Al₂O₃ (4 wt.% Au and 7.4 wt.% Au) catalysts and compared with the catalytic behaviour of Au/Co₃O₄/Al₂O₃ (4.1 wt.% Au) and Pt/Al₂O₃ (4.8 wt.% Pt) catalysts. The various characterization techniques employed (XRD, HRTEM, TPR and DR-UV–vis) revealed the presence of metallic gold, along with a highly dispersed CuO (6 wt.% CuO), or more crystalline CuO phase (12 wt.% CuO).

A higher CuO loading does not significantly influence the catalytic performance of the catalyst in propene oxidation, the gold loading appears to be more important. Moreover, it was found that 7.4Au/CuO/Al₂O₃ is almost as active as Pt/Al₂O₃, whereas Au/Co₃O₄/Al₂O₃ performs less than any of the CuO-containing gold-based catalysts.

The light-off temperature for C₃H₈ oxidation is significantly higher than for C₃H₆. For this reaction the particle size effect appears to prevail over the effect of gold loading. The most active catalysts are 4Au/CuO/Al₂O₃ (gold particles less than 3 nm) and 4Au/Co₃O₄/Al₂O₃ (gold particles less than 5 nm).

© 2005 Elsevier B.V. All rights reserved.

Keywords: Gold; Platinum; Additives; Copper oxide; Cobalt oxide; Propene and propane oxidation

1. Introduction

Catalytic combustion is an efficient way to control the emission of volatile organic compounds (VOCs). The most efficient catalysts belong to two categories: supported noble metal catalysts (Pd and Pt) and transition metal oxides (TMO), such as Cr, Fe and Mn oxide. The noble metal catalysts are more active, but rather unstable and expensive [1,2]. The use of TMO is an interesting alternative, especially from an economic point of view [3]. It has been established that TMO such as Co₃O₄, MgCr₂O₄ or Cr₂O₃ are very active as catalytic systems for hydrocarbon total oxidation [2,4,5]. Literature data suggest that CuO is less active for this kind of reactions [5]. The

mechanism of the total combustion of VOCs (propane, propene, acrolein, propan-2-ol and acetone) over Co₃O₄, MgCr₂O₄ and CuO was established to be of the Mars and van Krevelen type, and proceeds through the nucleophilic attack of the lattice oxygen of the above-mentioned oxides [5,6].

Recently, it was shown that highly dispersed gold-based catalysts on reducible metal oxides are extremely active for low temperature CO oxidation [7–9]. Other reactions where gold proved its efficiency as a catalyst include the total oxidation of VOCs [10–13]. The aim of the study described in the present paper is to compare the performance of CuO, Au and that of multicomponent Au–CuO catalysts for oxidation of propene as a typical component of VOCs emission. In addition, the catalytic performance of the above-mentioned catalysts have been compared with those of Au/Co₃O₄/Al₂O₃ and Pt/Al₂O₃. Both catalysts have been reported as being extremely active in total oxidation of propene [13,14]. In addition, total oxidation

* Corresponding author. Tel.: +31 71 527 4545; fax: +31 71 527 4451.

E-mail address: b.nieuwe@chem.leidenuniv.nl (B.E. Nieuwenhuys).

of C_3H_8 was measured over the above-mentioned catalysts and compared with $Au/Co_3O_4/Al_2O_3$ and Pt/Al_2O_3 . The reason was that Au/Co_3O_4 (10 wt.% Au) was reported to be a very efficient catalyst for total oxidation of saturated hydrocarbons (CH_4 and C_3H_8) [13], even exceeding the performance of 1 wt.% Pt/Al_2O_3 or 1 wt.% Pd/Al_2O_3 , whereas for propene oxidation, Pt/Al_2O_3 was reported to be superior to Au/Co_3O_4 [13].

2. Experimental procedures

2.1. Catalyst preparation

CuO/Al_2O_3 with two different Cu:Al atomic ratios were prepared by vacuum impregnation of $\gamma-Al_2O_3$ (Engelhard Al-4172P, $S_{BET} = 275 \text{ m}^2 \text{ g}^{-1}$) with $Cu(NO_3)_2 \cdot 3H_2O$ (Aldrich product, >99.9% purity). After drying for at least 16 h at 80°C in static air, the samples were calcined at 350°C for 2 h. These samples will be denoted as CuO-A (6 wt.% CuO) and CuO-B (12 wt.% CuO). Co_3O_4/Al_2O_3 (atomic ratio Co:Al = 1:15) was prepared using a similar approach.

Gold was added to Al_2O_3 or MO_x/Al_2O_3 (M: Cu and Co) via homogeneous deposition precipitation with urea [15]. The support (either pure alumina or MO_x/Al_2O_3) was immersed in water together with the corresponding solution of $HAuCl_4 \cdot 3H_2O$ and urea in excess. The mixture was warmed up to 80°C under vigorous stirring. The final pH of the solution was 8.5. A slow decomposition of urea ensures the deposition of gold mainly on the support, as relatively small particles. After several hours, the precipitate was thoroughly washed with hot water to remove chlorine, dried in static air for 16 h at 80°C and then calcined in O_2 at 300°C for 2 h. Table 1 collects the relevant data concerning the chemical composition of the catalysts used in this study.

Pt/Al_2O_3 was prepared by impregnation of the support with the corresponding solution of H_2PtCl_6 . The final noble metal loading was 4.8 wt.% Pt. The next steps included, similar as for the gold-based catalysts, drying and calcination at 300°C .

2.2. Catalyst characterization

To obtain structural/chemical information about the fresh and spent catalysts, various techniques have been used, including: atomic absorption spectroscopy (AAS), total surface

area (BET) determination, X-ray diffraction (XRD), high-resolution transmission electron microscopy (HRTEM), diffuse-reflectance UV–vis spectroscopy and temperature programmed reduction (TPR). A detailed description of the experimental procedures used for measurements have been reported earlier [12,15].

For TPR measurements the reducing gas (5 vol.% H_2 in Ar) passed with a flow rate of 30 ml min^{-1} through the catalyst bed at a heating ramp of 5°C min^{-1} . Prior to each experiment the sample was heated in an Ar flow at 100°C in order to eliminate the physically adsorbed water. A cold trap was mounted before the detector (TCD), which was used to monitor the rate of hydrogen consumption.

2.3. Catalytic activity measurements

Oxidation of the hydrocarbons was carried out in a lab-scale fixed bed reactor in which typically 0.2 g of catalyst was loaded and a total flow of 30 ml min^{-1} passed through the catalyst bed. All the gases used were 4 vol.% in He and the volumetric ratio used for the catalytic combustion of propene was $C_3H_6/O_2 = 1/9$ and for propane $C_3H_8/O_2 = 1/16$. Prior to each experiment, the catalyst was reactivated in situ (300°C) in hydrogen. The gas flow was adjusted by mass flow controllers and the outlet stream was analyzed by means of a mass spectrometer. The experiments were performed in a temperature programmed way and consisted of at least four heating–cooling cycles between room temperature and 400°C . To compare the catalytic performance of the catalysts tested in this study, the conversion achieved during the second heating cycle is used. Results obtained for the third and further cycles were similar to those found for the second cycle.

3. Results and discussions

3.1. Characterization

The results are summarized in Table 1. It should be mentioned that the concentration of CuO for Au–CuO-A and Au–CuO-B, as determined by AAS, was within experimental error the same as the CuO loading prior to Au deposition. The various characterization techniques employed (XRD, HRTEM, TPR and DR-UV–vis) revealed the presence of metallic gold,

Table 1
Catalyst characterization by means of atomic absorption spectroscopy AAS, BET, XRD, HRTEM

Catalyst	Component content (wt.%)		XRD			HRTEM		BET surface area ($\text{m}^2 \text{ g}^{-1}$)
	Au	CuO	d_{Au} (nm)	d_{Au} (nm)	S_{Au} ($\text{m}^2 \text{ g}^{-1}$)	d_{Au} (nm)	D (%)	
Au–CuO-A	4	5.9	3.0 ± 0.1	3.1 ± 0.2	2.77	2.3 ± 0.2	30	253
Au–CuO-B	7.4	12	6.8 ± 0.2	7.0 ± 0.1	2.74	n.m.	–	212
$Au/Co_3O_4/Al_2O_3$	4.3	–	5.0 ± 0.1	5.9 ± 0.1	2.22	9.9 ± 0.2	5	207
Au/Al_2O_3	4.1	–	4.3 ± 0.1	4.5 ± 0.2	2.4	5.2 ± 0.2	11.5	260
CuO-A	–	6	–	–	–	–	–	225
CuO-B	–	12	–	–	–	–	–	200

d_{Au} : Mean diameter of gold particles, fresh catalysts; d_{Au} : mean diameter of gold particles, spent catalysts (C_3H_6 oxidation); S_{Au} : gold surface area, XRD; D : gold dispersion, HRTEM; n.m.: not measured.

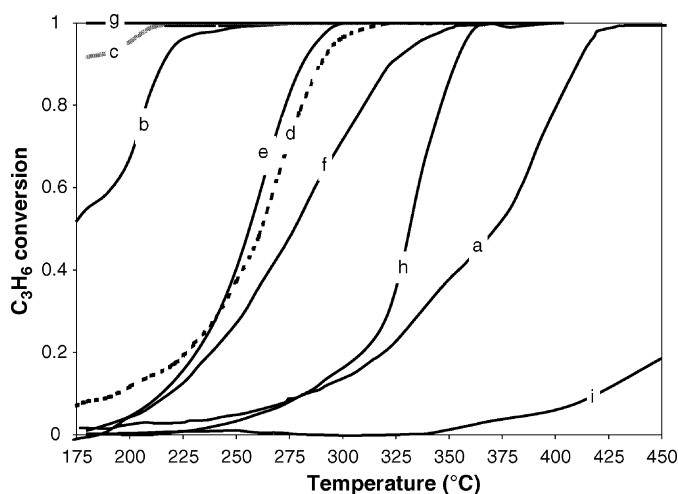


Fig. 1. Propene conversion vs. temperature over: (a) Au/Al₂O₃, (b) Au–CuO–A, (c) Au–CuO–B, (d) CuO–A, (e) CuO–B, (f) Au/Co₃O₄/Al₂O₃, (g) Pt/Al₂O₃, (h) Co₃O₄/Al₂O₃, and (i) Al₂O₃. The volumetric reactant ratio: C₃H₆/O₂ = 1/9.

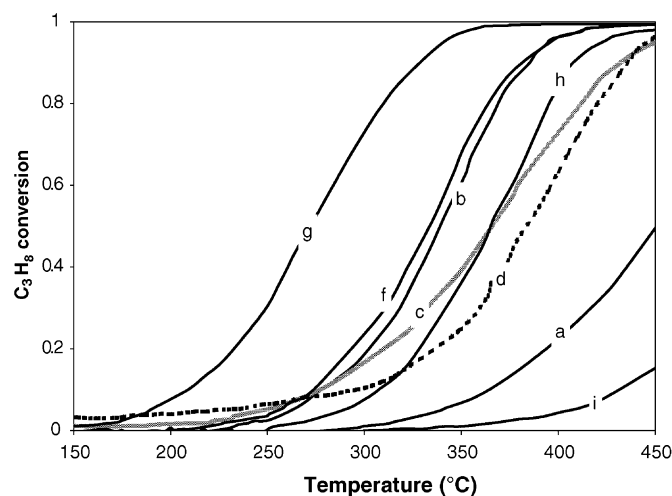


Fig. 2. Propane conversion vs. temperature over: (a) Au/Al₂O₃, (b) Au–CuO–A, (c) Au–CuO–B, (d) CuO–A, (f) Au/Co₃O₄/Al₂O₃, (g) Pt/Al₂O₃, (h) Co₃O₄/Al₂O₃, and (i) Al₂O₃. The volumetric reactant ratio: C₃H₈/O₂ = 1/16.

along with a highly dispersed CuO (6 wt.% CuO), or more crystalline CuO phase (12 wt.% CuO). The diffraction line of Au from $2\theta = 38.2^\circ$ was used to estimate the average gold particle size, using the Scherrer equation. The results obtained from XRD have also been used to estimate the metallic surface area of gold (Table 1). The calculations have been made by assuming that the gold particles are hemispherical in shape with the flat side on the support, according to the following formula:

$$S_{\text{Au}} = \frac{50\,000W}{\rho d} \quad (1)$$

where W corresponds to the gold loading, ρ is the density of gold ($19.3\text{ cm}^3\text{ g}^{-1}$) and d is the diameter of gold particles as determined by XRD (Å).

In general the shape of the gold particles visualized by HRTEM was hemispherical and no direct influence of CuO or Co₃O₄ on the shape of the Au particles was found. The average size of the gold particles varied between 2.3 nm (Au–CuO–A) and 9.9 nm (Au/Co₃O₄/Al₂O₃). However, the latter catalyst displayed also very small gold particles, around 2 nm.

3.2. Catalytic activity measurements

The catalytic activity results of the gold-based catalysts and the corresponding supports are presented in Fig. 1 in terms of propene conversion versus temperature. Au/Al₂O₃ (curve a, Fig. 1) is less active than CuO/Al₂O₃ (curves d and e). On the other hand, the catalytic activity of CuO–B (curve e) with its higher loading is only slightly higher than that of CuO–A (curve d).

A strong synergistic effect was found by combining Au and CuO (curves b and c). However, Au–CuO–B (curve c) appears to be more active than Au–CuO–A (curve b). The Au surface area (Table 1) is similar for both CuO-containing gold-based catalysts and higher than that of Au/Al₂O₃ or Au/Co₃O₄/Al₂O₃. This suggests that the superior catalytic activity found for Au–CuO–B may have another origin than that of metallic surface

area. Moreover, the high catalytic activity found for Au–CuO–B may also imply that the particle size effect may not be that crucial, once an additive with intrinsic catalytic activity is added to Au. Thus, in particular the gold loading appears to play an important role in propene oxidation. Analysis of spent catalysts following a full reaction cycle of more than 10 h (see Table 1) provided evidence for the existence of relatively stable Au particles.

It has been previously reported that gold deposited on Co₃O₄ (10 wt.% Au) exhibits the highest catalytic activity for the complete oxidation of C₃H₈ and CH₄ among several gold-based catalysts, Pt/Al₂O₃ (1 wt.% Pt) and Pd/Al₂O₃ (1 wt.% Pd) [13,16]. On the other hand, it was reported that Au/Co₃O₄ was inferior to Pt and Pd deposited on alumina for the combustion of unsaturated hydrocarbons such as propene. In this study, we have compared the catalytic performance of Au–CuO–A and Au–CuO–B with that of Au/Co₃O₄/Al₂O₃ (4.3 wt.% Au, curve f in Fig. 1) and Pt/Al₂O₃ (4.8 wt.% Pt, curve g in Fig. 1) for total oxidation of propene.

A similar comparative study was carried out for total oxidation of C₃H₈. The results are presented in Fig. 2 and discussed below. Contrary to earlier reports [13,16], Pt/Al₂O₃ is the best catalyst for both oxidation reactions, if a similar noble metal loading is used. Moreover, Au/Co₃O₄/Al₂O₃ is less active than any of the CuO-containing gold-based catalysts (curve f, Fig. 1). To oxidize propane, a higher temperature is required (Fig. 2). The synergistic effect found for C₃H₆ oxidation by combining Au and CuO is also found for C₃H₈ oxidation. However, the catalytic performance of Au/Co₃O₄/Al₂O₃ (curve f, Fig. 2) is nearly the same as that of Au–CuO–A (curve b, Fig. 2). This can be explained by considering the concurrent effect of two different factors: the presence of gold nanoparticles and the identity of the additives. XRD and HRTEM results (Table 1) detected smaller Au particles for Au–CuO–A than for Au/Co₃O₄/Al₂O₃. Consequently, the estimated metallic surface area is larger for Au–CuO–A. A similar trend is observed when the dispersion of the above-mentioned Au–

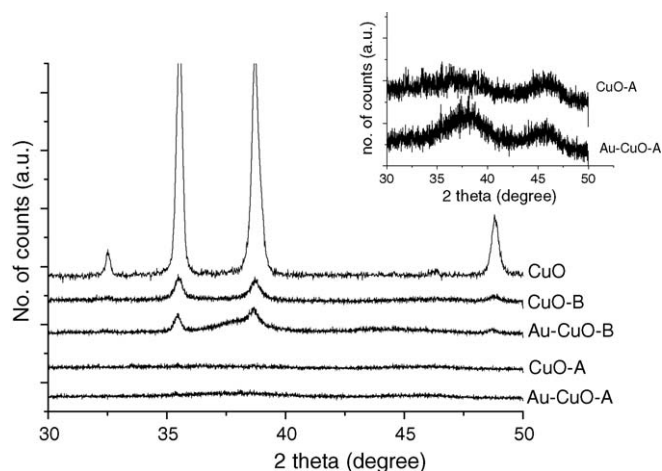


Fig. 3. XRD patterns of CuO, Au–CuO-A, Au–CuO-B and the corresponding supports.

based catalysts is considered. On the other hand, the results shown in Fig. 2 clearly indicate that $\text{Co}_3\text{O}_4/\text{Al}_2\text{O}_3$ is more active than CuO-A. In this view it appears that not only small Au particles are very important, but also the identity of the additive. A higher loading (either Au or CuO) does not improve the catalytic performance (curve c, Fig. 2).

The higher temperature needed to oxidize propane, as compared to propene, can be easily understood on the basis of the generally higher activity of alkenes compared to alkanes. On the other hand, it is interesting to note that a different order in activity of the catalysts was found for propane and propene oxidation.

Previous studies showed that C_3H_6 can interact with Au(111) and Au(100) surfaces via its π bond [17]. The activation of oxygen is a difficult step on gold surfaces [16]. It has been reported that the oxygen needed to oxidize propene can be provided by TMO additives, via a Mars and van Krevelen type of mechanism [12]. The data presented above may suggest that the activation of O_2 is better achieved by the Au–CuO system than by the Au– Co_3O_4 . This activation is probably related to the ability of the additives in supplying the active oxygen during the catalytic reaction.

The formation of the crystalline CuO phase is detected by XRD for CuO-B and Au–CuO-B (Fig. 3). The pattern of crystalline CuO is hardly visible for CuO-A and Au–CuO-A and the peak intensity of $2\theta = 38.2^\circ$ increases after gold deposition (Au–CuO-A). These results indicate that the structure of CuO may be important and a more crystalline copper oxide system (Au–CuO-B and CuO-B) may improve the catalytic activity.

The different order in catalytic activity in propane and propene oxidation is not yet understood. It is possible that the activation of propane proceeds more easily on smaller Au particles than on larger ones. It is well known that smaller gold particles are able to activate different kinds of reactants more easily. In our opinion this is a result of the high fraction of corners, edges and kinks on small crystallites [16,18,19], or more general, the increased concentration of low coordinated surface atoms.

4. Conclusions

The catalytic oxidation of saturated (propane) and unsaturated (propene) hydrocarbons has been studied over various gold-based catalysts. A strong synergistic effect was found by combining Au with CuO or Co_3O_4 . The beneficial effect of Co_3O_4 addition is less pronounced for C_3H_6 oxidation, but it is large for propane oxidation. The bicomponent Au–Cu containing catalysts perform well in both reactions. However, $\text{Pt}/\text{Al}_2\text{O}_3$ exhibits a higher activity than the Au containing catalysts. The gold particle size effect is of crucial importance for propane oxidation and less relevant for propene oxidation.

Acknowledgments

A.C. Gluhoi would like to express her gratitude to Dr. P. Marginean for fruitful discussions and to F. Ruiz Medina and E. Flores for technical support. The Netherlands Organization for Scientific Research, NWO (Grant NWO/CW 99037 and NWO #047.015.003) and Mexican grants (UNAM COIC-OAI-174-04, IN109003 and CONACYT No. 42568-Q) are gratefully acknowledged for financial support.

References

- [1] J.N. Armor (Ed.), *Environmental Catalysis*, vol. ACS Symp. Ser. 552, American Chemical Society, Washington, DC, 1994.
- [2] G.K. Borekov, *Catalysis Science and Technology*, vol. 3, Springer-Verlag, Berlin, 1985.
- [3] M.F.M. Zwinkels, S.G. Jaras, P.G. Menon, T.A. Griffin, *Catal. Rev. Sci. Eng.* 35 (1993) 319.
- [4] E. Finocchio, G. Busca, V. Lorenzelli, *J. Chem. Soc., Faraday Trans.* 90 (1994) 3347.
- [5] E. Finocchio, R.J. Willey, G. Busca, V. Lorenzelli, *J. Chem. Soc., Faraday Trans.* 93 (1997) 175.
- [6] E. Finocchio, G. Busca, V. Lorenzelli, V.S. Escibano, *J. Chem. Soc. Faraday Trans.* 92 (1996) 1587.
- [7] M. Haruta, N. Yamada, T. Kobayashi, S. Iijima, *J. Catal.* 115 (1989) 301.
- [8] S.D. Gardner, G.B. Hoflund, B.T. Upchurch, D.R. Schryer, E.J. Kielin, *J. Schryer, J. Catal.* 129 (1991) 114.
- [9] S.D. Lin, M. Bollinger, M.A. Vannice, *Catal. Lett.* 17 (1993) 245.
- [10] S. Minico, S. Scire, C. Crisafulli, R. Maggiore, S. Galvagno, *Appl. Catal. B* 28 (2000) 245.
- [11] S. Scire, S. Minico, C. Crisafulli, C. Satriano, A. Pistone, *Appl. Catal. B* 40 (2003) 43.
- [12] A.C. Gluhoi, N. Bogdanchikova, B.E. Nieuwenhuys, *J. Catal.* 229 (2005) 154.
- [13] M. Haruta, *Catal. Today* 36 (1997) 153.
- [14] A.C. Gluhoi, N. Bogdanchikova, B.E. Nieuwenhuys, *J. Catal.* 229 (2005) 154.
- [15] A.C. Gluhoi, M.A.P. Dekkers, B.E. Nieuwenhuys, *J. Catal.* 219 (2003) 197.
- [16] G.C. Bond, D.T. Thompson, *Catal. Rev. Sci. Eng.* 41 (1999) 319.
- [17] K.A. Davis, D.W. Goodman, *J. Phys. Chem. B* 104 (2000) 8557.
- [18] N. Lopez, J.K. Norskov, T.V.W. Janssens, A. Carlsson, A. Puig-Molina, B.S. Clausen, J.D. Grunwaldt, *J. Catal.* 225 (2004) 86.
- [19] C.P. Vinod, J.W. Niemantsverdriet, B.E. Nieuwenhuys, *Appl. Catal. A* 291 (2005) 93.